

Supplementary Information

SI 1. Digital programming principles of Hexadecimal (HEX) sequencer

In DPFS, the digital controller controls its connected twelve solenoid valves (V1-V12) through the digital code in the Hexadecimal (HEX) sequencer. The encoding in the HEX sequencer is determined by the binary value Y , and the execution time can be set on demand. The value of Y is decided by $Y = \sum 2^{(N-1)}$, where N is the internal number of the valves. For example, when valves V1, V2, V7 and V8 are opened, those remaining ones closed and the $Y = 2^{1-1} + 2^{2-1} + 2^{7-1} + 2^{8-1} = 195$. If the value status lasts for 120 ms, the corresponding 'setting time' in HEX sequencer is set as 120 ms.

SI 2. EAV preparation and characterization

Template perfusion method¹ was used to prepare EAVs and the specific process is shown in Fig. S1A. First, a rigid polypropylene plastic tube (blue) was selected with a length of 6 cm, an inner diameter of 3.5 mm, and an outer diameter of 6.35 mm, and a stainless steel metal rod (gray) with an outer diameter of 2.5 mm as molds. After that, they were soaked in white oil (10# food grade, Shanghai Xiangping Industrial Co., Ltd., China) for 1H to ensure that the inner wall of the produced EAV was smooth. In second step, one end of the plastic tube was fixed with a template holder, and then the rigid plastic tube was filled with PDMS pre-polymer solution (sylgard gel and elastomer (Dow Corning, USA) mixed at a mass ratio of 10: 1) by a syringe pump. Then, the metal rod was slowly inserted into the plastic tube center, and then the template holder was used to hold the other end of the rigid plastic tube so that the relative position with the metal rod remained unchanged (as shown in Fig. S1B). Third, the entire device was placed in an 80 °C oven for 2H to cure and a transparent EAV was obtained after demolding (as shown in Fig. S1C). Finally, the EAV was put into 10% sodium dodecyl sulfate solution (AR, Shanghai McLean Biochemical Technology Co., Ltd., China) to remove the remaining white oil, and then was rinsed with 75.0% ethanol. EAV is then dried and put in a sterile environment, ready for use.

A field emission scanning electron microscopy (MIRA 3 FE-SEM, TESCAN, Czech) was used to inspect the morphology and the inner wall smoothness of the prepared EAV. The inset in Fig. S1C is an enlarged picture demonstrating the partial section of the inner wall in the EAV tube. It can be seen

that the inner wall is uniform and smooth, which ensures the consistency of the culture environment for HUVEC in different EAV sections.

Previous studies has shown that elastic fibers are one of the main components of the blood vessel wall^{2,3}. The shorter distance it is to the heart location, the higher the proportion of elastic fibers in the arterial blood vessel wall and the better compliance of the blood vessels will be. In normal circumstances, the Young's modulus of elastic fibers is about $3.0 \times 10^5 \sim 6.0 \times 10^5 \text{Pa}$ (as illustrated in the pink rectangular area in Fig. S1D)⁴. In our experiment, the young's modulus of EAV was measured by a nano indenter (Optics 11, Netherlands) and the value was 383.0KPa, which is consistent with the Young's modulus of the real elastic fiber. It indicates that the EAV prepared in this experiment has a comparable bionic to *in vivo* vessels.

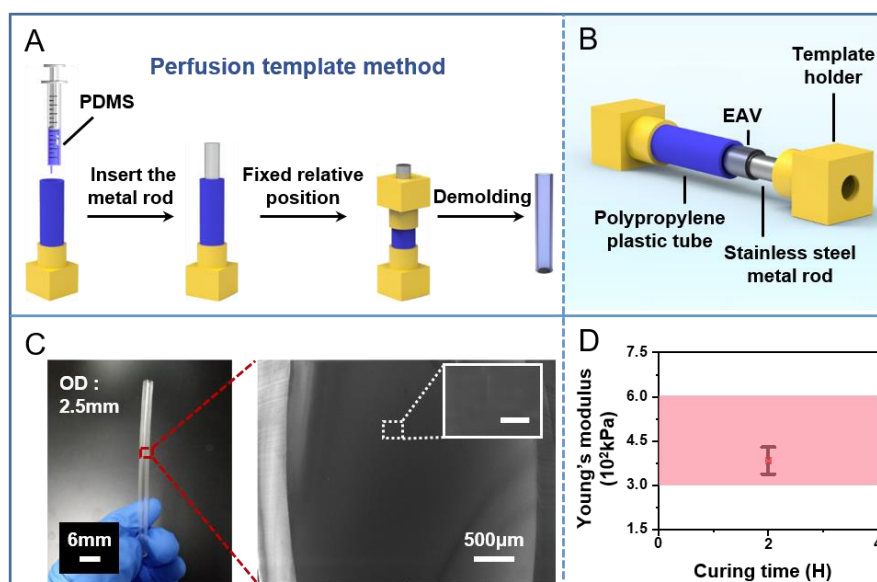


Fig. S1 (A) Schematic diagram of the process of EAV preparation based on perfusion template method. (B) Illustration of template structure. (C) The picture on the left shows the hollow EAV prepared via the template method. The right shows the structural morphology of the inner EAV wall with FE-SEM. The enlarged upper-right inset indicates its smoothness (scale bar=10μm). (D) The comparison of Young's modulus between EAV and elastic fibers (pink area) indicates that the EAV has favorable bionic properties.

SI 3. Flow characteristics of single paired solenoid valves

The digital controller of the DPFS contains a pulse generator and a HEX sequencer to control the working state of the solenoid valve. The pulse generator controls the working state and working time

of all solenoid valves at the same time, while the HEX sequencer independently controls the working state and working time of each solenoid valve. Therefore, in the experiment we selected the HEX sequencer to control the solenoid valve to realize the simulation of the human left coronary blood flow curve in vitro. The flow characteristics of EAV controlled by a single paired of solenoid valves in the DPFS was explored. The HEX sequencer was set according to the command in Fig. S2A. The working conditions of the solenoid valves V1 and V7 and the corresponding flow result provided a reference for the subsequent further simulation of the human left coronary blood flow curve.

The working status of the solenoid valve in the DPFS and the corresponding EAV flow changes are as follows. First, the solenoid valve V1 is opened, the solenoid valve V7 is closed, and the execution time is 0.5s. The fluid passes through V1 and EAV and is blocked by V7. At the instant of V1 opening, the flow rate in EAV increases in a short time (P1-P2 phase, the time interval is about 0.1s). When the flow rate reaches the maximum value, fluctuate happens due to the continuous fluid flow driven by the peristaltic pump, and this state continues for a period of time (P2-P3 stage, the time interval is about 0.412s). Second, the solenoid valve V1 is closed, the solenoid valve V7 is open and the execution time is 0.5s. The fluid is blocked by V1, but it can flow out of V7. The EAV flow rate decreases (P3-P4 stage, time interval is about 0.101s). When the fluid flow reaches the minimum value, it fluctuates within a certain range and lasts for a period of time (P4-P5 stage in Fig. S2B, time interval is about 0.404s).

In this way, the actual fluid curve under the control of a single paired of solenoid valves in Fig. S2B was obtained. The actual flow waveform was similar to the waveform generated by a rectangular pulse. But it is noted that the period (1.00s) was slightly different from the period of the program command (1.02s), which may be caused by the delayed time response of the solenoid valve.

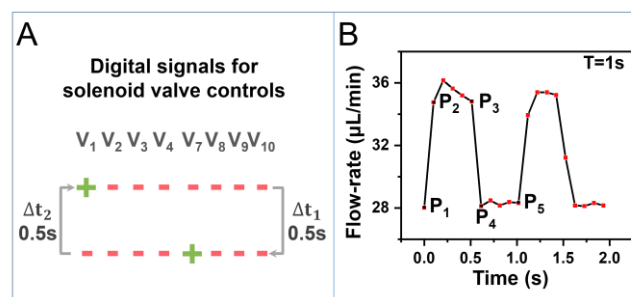


Fig. S2 (A) The signal commands of valve controller for a single pulse fluid. V1-V4 and V7-V10

respectively represent the upstream and downstream valve groups respectively. '+' represents the solenoid valve is open and the fluid can pass. '-' indicates the solenoid valve is closed and blocks the fluid, the duration is 0.5 s. (B) The actual flow curve measured in the EAV. The time intervals corresponding to the four stages of P1P2, P2P3, P3P4 and P4P5 are 0.1 s, 0.412 s, 0.101 s and 0.404 s respectively, where the period is about 1 s and the peristaltic pump flow rate is 50 $\mu\text{L}/\text{min}$.

SI 4. The principle of EAV flow with solenoid valve controls for simulations of the blood flow curve in the human left coronary artery

On the basis of SI 3, we have repeatedly debugged the program to obtain a decent program command to simulate the blood flow curve in the left coronary artery in EAVs. The specific formation process is as follows.

(1) The programming principle for different waveform curves.

When the number of on-off solenoid valves is different, the flow rate in EAV also varies. That is, in the DPFS, if four solenoid valves are opened in the upstream, larger flow rate would be obtained than merely single solenoid valve is opened. According to this characteristic and in combination with the flow curve shown in Fig. 2D, i. e., the characters of experiencing a large peak first and followed by a small peak, the experiment had employed the solenoid valves V1-V4 at the EAV upstream and simultaneously placed the solenoid valves V7-V8 at downstream of the EAV. Two sets of solenoid valves with different valve numbers coordinated and operated alternately to achieve two peak waveforms. The function time of the solenoid valves also corresponded to the interval between the rise and fall of the two peak waveforms. Specifically, the rising (time interval Δt_1) of the large peak waveform in Fig. 2D was realized by the upstream solenoid valves V1-V4, and the falling (time interval Δt_2) of the waveform was realized by the downstream solenoid valves V7-V10. The rising (time interval Δt_3) of the small peak waveform in Fig. 2D was realized by the upstream solenoid valve V1 alone, and the falling (time interval Δt_4) of the waveform was realized by the downstream solenoid valve V7 alone. In general, the working time of the solenoid valve corresponded to the time interval of the waveform.

(2) The programming process.

Corresponding to the major peak waveforms in Fig. 2D, First, the rising of the waveform was realized by the joint upstream solenoid valves V1-V4. $Y_1 = 2^{1-1} + 2^{2-1} + 2^{3-1} + 2^{4-1} = 15$ and the

execution time of the current state is $\Delta t_1 = 0.160\text{s}$. After that, the descent waveform was coordinately realized by upstream solenoid valves V7-V10. The corresponding $Y_1 = 2^{7-1} + 2^{8-1} + 2^{9-1} + 2^{10-1} = 960$ and the execution time of this state is $\Delta t_2 = 0.340\text{s}$. The realization procedure of the small peak waveforms in Fig. 2D was similar to the above one. At the beginning for the rising waveform, $Y_3 = 1$ and the execution time is 0.140s . For the falling waveform, $Y_4 = 64$ and the execution time is 0.100s .

SI 5. Finite element analysis (FEA) of the flow and the pressure field inside the EAV

The EAV shape would deform and contract as a result of periodic flow. Hence, the fluid-solid coupled finite element simulation was performed to analyze the flow field and wall stress in EAV. First, the shape and structure of the EAV was regarded as a combination of Bezier polygons. It was divided into two areas and namely the fluid area and the wall zone. The fluid was set as incompressible Newtonian fluid, the density was set to $1.0 \times 10^3 \text{ kg/m}^3$, and laminar flow condition was considered with a Reynolds number of 0.33. The EAV wall was an isotropic linear elastic material with a density of 970 kg/m^3 , a Young's modulus of 750 kPa , and a Poisson's ratio of 0.49. Second, fixed constraints on the inlet and outlet of the pipe wall were imposed and the length of the inlet and outlet were both set to be 1.0 m . The inlet flow rate of the pulse fluid in the EAV was determined by the first four components with the largest amplitudes after the Fourier transform of the actual flow curve (Fig. 3B). Besides, it was assumed that the fluid and the EAV wall met the no-slip boundary condition. Furthermore, the fluid and the wall area were meshed where the cell size was set to normal, the simulation time was 2.0 s , and the time step was set to 0.01 s . Through the COMSOL program calculations, the fluid velocity distribution in the EAV, as well as the stress distribution in the pipe wall at different times were obtained and demonstrated in Fig. 4B.

SI 6. Procedure for calculating the HUVEC average fluorescent intensity (CAFI)

In order to quantify the spatial-temporal proliferation of HUVEC, the HUVEC CAFI was calculated to indicate cell proliferation indirectly. First, the fluorescence image of HUVEC was acquired at regular intervals using an inverted fluorescence microscope (Ti-E, Nikon, Japan). The central area of image was then equally divided into 21 regions with a length of 1 mm and a width of 0.6 mm , as is shown in Fig. S 3. Second, the image was gray-processed (white gray value is 255, black gray value is 0) by MATLAB

R2017a software (Math Works, USA), and then the gray value of per pixels in each region was analyzed to calculate its average value $\overline{\text{Gray}}$, i. e.,

$$\overline{\text{Gray}} = \frac{\sum \text{Gray}_i}{n}$$

where $i=1, 2, 3 \dots n$, n is the sum of pixel numbers in each region.

Finally, based on the data obtained above, the 3-D spatial and temporal distribution of HUVEC CAFI were plotted by Origin2017 software.

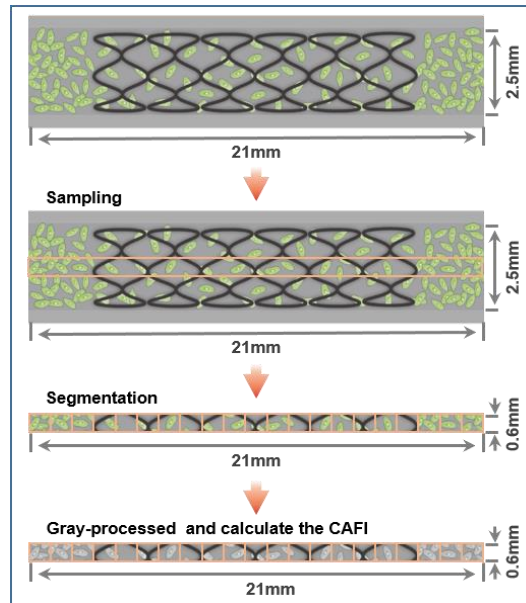


Fig. S3 Schematic diagram of calculating the HUVEC average fluorescent intensity (CAFI). First, the fluorescence image of HUVEC was intercepted and divided into 21 regions with a length of 1.0 mm and a width of 0.6 mm. Then, the image was gray-processed and the average value $\overline{\text{Gray}}$ of each region was calculated by MATLAB R2017a software (Math Works, USA).

SI 7. Procedure for implanting BMS and DES into the EAV

In order to establish an in vitro experimental model that approaches the microenvironment of the blood vessel implanted with stent to investigate the interaction between HUVEC and stent influence, the EAV containing BMS and DES had been prepared in the following procedures. First, the stent with a compression balloon was inserted into the EAV, and then connected to a pressure pump. Then, the air was repeatedly pumped into the compression balloon until the pressure was not less than 3 atm. At that time, the stent would be expanded with the expansion of the compression balloon. After that, the air was evacuated to remove the compression balloon slowly and smoothly. The stent

had been tightly attached to the inner wall of the EAV.

SI 8. HUVECs immunofluorescence analysis

For the cell immobilization process, the medium was removed from the EAV. Then, the EAV was filled with PBS and kept still for 15 min before aspiration. This operation was repeated three times until the previous culture medium was completely removed. Next, 4.0% paraformaldehyde (Beyotime, MA, USA) fulfilled the EAV and maintained for 15 min at 4.0 °C in order to fix HUVECs, before the EAV was rinsed by PBS again for three times. Following that, 0.5% (v/v) Triton X 100 (Sigma, USA) was used to treat permeability of cell membrane for 30 min, and then rinsed by PBS for three times. 10.0% goat serum was used for cell blocking. After that, the primary antibody Rabbit Anti-VE Cadherin Ployclonal Antibody (Cell Signalling Technology, MA, USA) for VE-Cadherin was diluted with PBS at 1:100 ratio, and for the next 12 h the diluted primary antibody solution was introduced into the EAV at 4.0 °C. Then, the EAV was washed thoroughly with PBS for three times to complete the target protein labelling. Then, the secondary antibody, streptavidin-Alexa Fluor 647 antibody (Bioss, China), was diluted with PBS at 1:750 ratio and fulfilled the EAV, which was then kept at 37.0 °C in the dark for 12 h. Subsequently, the secondary antibody solution was removed, and the EAV was cleaned with PBS for three times. For vWF staining, the primary antibody, Rabbit Anti-VWF Ployclonal Antibody (Cell Signalling Technology, MA, USA), and the secondary antibody, streptavidin-Alexa Fluor 555 antibody (Bioss, China), were used as described above. Besides that, DAPI solution (Solarbio, China) was introduced in EAV for 10 min as to stain nuclear of HUVECs.

In order to analyze the growth of HUVECs in EAVs under pulse flow controlled by DPFS, the cells had been continuously cultured for 24 h and the two-photon confocal microscope (SP8, Leica, Germany) had been used for 3-D image analysis (Fig. S4A and Fig. S4B). The pictures demonstrate the 3-D profiles of the cell layer that attached to the EAVs inner wall. The overall thickness of the cell layer was about 25 μ m and indicated that HUVECs formed mono-layer in EAVs.

Furthermore, the HUVECs were labeled by immunofluorescence staining and imaged by the two-photon confocal microscope as to illustrate their healthiness after pulse flow application. In details, the HUVECs in EAVs *in situ* were able to successfully express GFP after transfection with CD513B and nuclear exhibit normal morphology after staining with DAPI. In addition to that, the immunofluorescence revealed that, both vascular endothelial cadherin (VE-cad) and von Willebrand

factor (vWF) have normal expressions. These results indicate that HUVECs in EAVs not only have good conditions, but also their widely expressed VE-cad and vWF are able to participate cell-cell interaction, transmit relative signals as well as facilitate vascular remodeling and maintenance of vascular integrity.

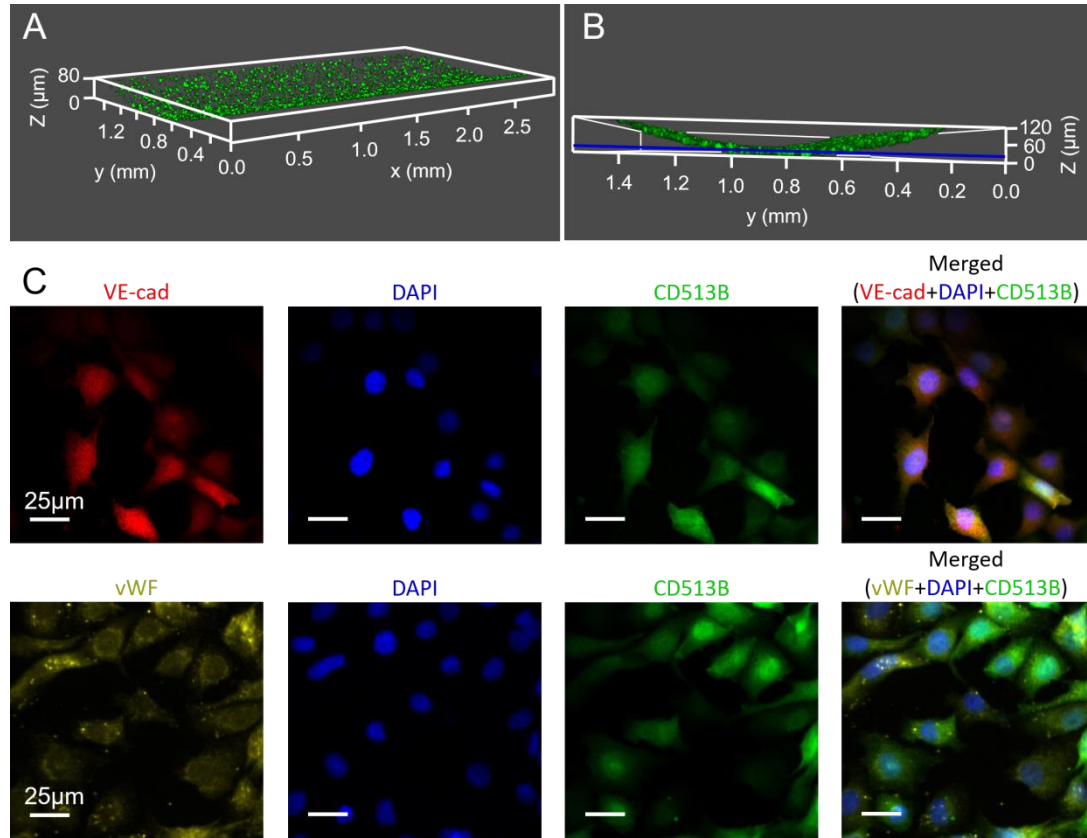


Fig. S4 The growth morphology and protein analysis of HUVECs in EAV under pulse flow condition. (A-B) the side view and front view of 3-D construction of the confocal microscopy, which indicate that HUVECs layer was a mono-layer with about 25 μm thickness. (C) The immunofluorescence analysis: VE-cad (red), DAPI (blue), CD513B (green), vWF (yellow).

SI 8. Measurement method of NOS in HUVEC

In order to assess the postoperative risk associated with stenting, the likelihood of vasospasm could be indirectly judged by measuring the NOS in HUVEC. First, the HUVEC cultured for 192H under pulse flow condition were digested with trypsin and stored in a 1.5ml centrifuge tube. Then, the supernatant was removed by centrifugation and 200μL Pipazetate Hydrochloride containing 1mM of Phenylmethanesulfonyl fluoride was added to cleave the cells. After that, the sample was centrifuged for 5 min and the supernatant was treated with a human nitric oxide synthase ELISA kit, and its OD value was measured at 450nm using an enzyme label analyzer (Rayto rt-6100, Shenzhen Leidu Life

Sciences co., LTD., CHINA). Finally, the concentration of NOS in HUVEC had been calculated by substituting the OD value into the standard curve equation.

SI 9. The original data images of HUVEC growth in EAV, EAV-BMS and EAV-DES under the static and pulse conditions, taken at every 24 hours.

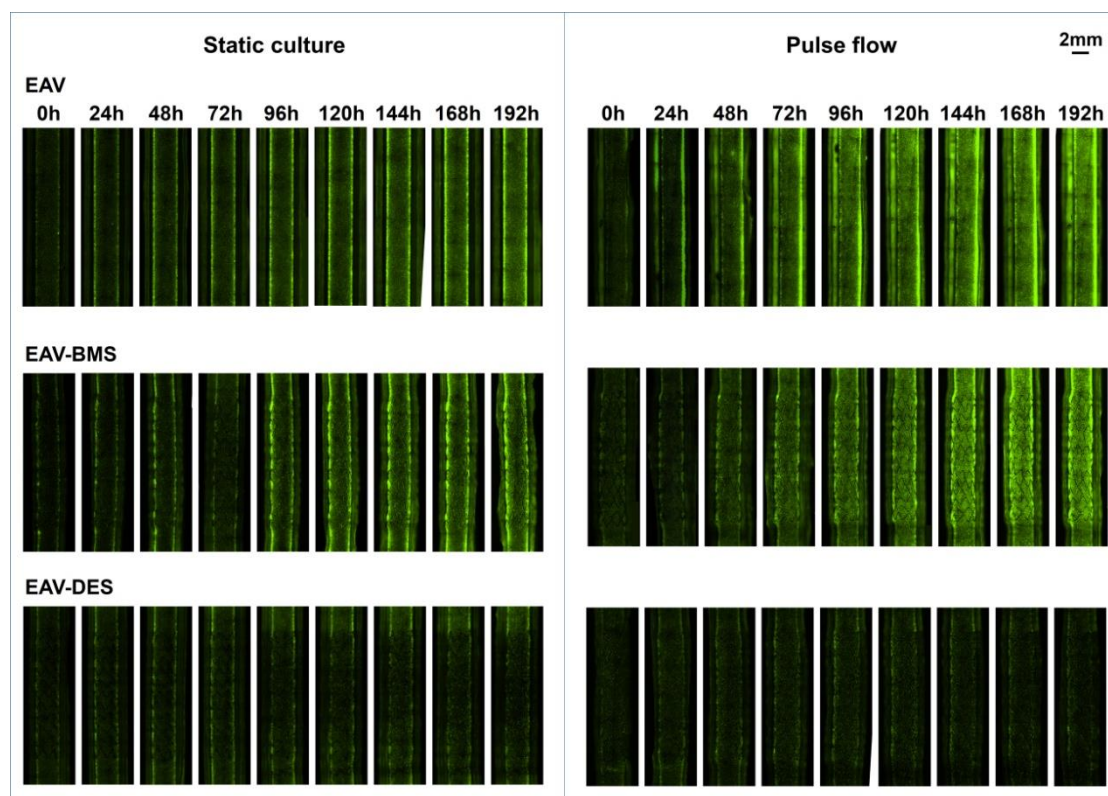


Fig. S5 the original fluorescent images of HUVECs in EAVs.

SI 10. EAVs elasticity observation

In order to visualize the elasticity of EAVs under pulse flow conditions, we have prepared an EAV with red fluorescent particles (RFP) fixed inside and employed Ti-E invert microscopy to record its transformation. In details, first the RFP particles with 1.0 μm diameter were uniformly mixed with PDMS, and EAV was prepared in the routine procedure. After that the EAV was connected with DPFS and operation was started. Movie S1 shows with the Ti-E microscope, the RFP particles exhibited obvious forward-backward motion and indicate the EAV has elastic property under pulse flow conditions.

References

1. W. J. Zhang, Y. S. Zhang, S. M. Bakht, J. Aleman, S. R. Shin, K. Yue, M. Sica, J. Ribas, M. Duchamp, J. Ju, R. B. Sadeghian, D. Kim, M. R. Dokmeci, A. Atala and A. Khademhosseini, Lab on a Chip, 2016, **16**, 1579-1586.
2. S. Sugita and T. Matsumoto, Biomech Model Mechanobiol, 2017, **16**, 763-773.
3. G. Vieira-Damiani, D. P. Ferro, R. L. Adam, A. A. D. Thomaz, V. Pelegati, C. L. Cesar and K. Metze, Elastic fibers and collagen distribution in human aorta, 2011, **7903**, 79030B.
4. X. Jia, Liaoning: Liaoning Technical University, 2002, 11-20.